

# Transition Onset Prediction for High-Speed Flow

R. D. McDaniel\*

*North Carolina State University, Raleigh, North Carolina 27695-7910*

R. P. Nance†

*U.S. Naval Surface Warfare Center, Dahlgren, Virginia 22448-5100*

and

H. A. Hassan‡

*North Carolina State University, Raleigh, North Carolina 27695-7910*

**An approach that treats nonturbulent fluctuations in a turbulencelike manner and determines onset and extent of transition as part of a flow calculation is used to study transition at high Mach numbers. Three sets of previously obtained experimental data involving straight and flared cones at zero angle of attack are used to calibrate and validate the model. Two sets, at Mach numbers 3.5 and 6, were carried out in quiet tunnels, and the third set was carried out at a Mach number of 8 in a conventional tunnel. The results suggest that the second mode is not the only mode responsible for transition at high Mach numbers. In general, fair to good agreement with measured recovery factors, adiabatic wall temperatures, and heat-transfer rates is indicated.**

## Nomenclature

$a$	= model constants (first mode)
$b$	= model constants (second mode)
$C_\mu$	= constant, 0.09
$k$	= fluctuating kinetic energy, $\text{m}^2/\text{s}^2$
$M$	= Mach number
$\bar{m}$	= rms of mass flux, $\text{kg}/\text{m}^2 \cdot \text{s}$
$\bar{m}$	= mean mass flux, $\text{kg}/\text{m}^2 \cdot \text{s}$
$P$	= pressure, Pa
$Q$	= mean velocity
$q$	= heat flux at the wall, $\text{W}/\text{m}^2$
$Re$	= Reynolds number
$R_T$	= parameter defined in Eq. (18)
$r$	= recovery factor
$s_{ij}$	= strain tensor, $\text{s}^{-1}$
$T$	= temperature, K
$Tu$	= turbulent intensity
$U_p$	= phase velocity, $\text{m}/\text{s}$
$\tilde{u}_i$	= mean velocity vector, $\text{m}/\text{s}$
$x_t$	= location of transition onset (m)
$\alpha$	= parameter defined in Eq. (17)
$\Gamma$	= intermittency
$\delta$	= boundary-layer thickness, m
$\delta^*$	= displacement thickness, m
$\zeta$	= enstrophy, $\text{s}^{-2}$
$\lambda$	= wavelength, m
$\mu$	= viscosity, $\text{kg}/\text{m} \cdot \text{s}$
$\nu$	= kinematic viscosity, $\text{m}^2/\text{s}$
$\xi$	= parameter defined in Eq. (16)
$\rho$	= density, $\text{kg}/\text{m}^3$
$\tau$	= timescale, s
$\tau_k$	= decay time, s
$\psi$	= direction of wave number, deg
$\omega$	= frequency, $\text{s}^{-1}$

## Subscripts

aw	= adiabatic wall
$e$	= boundary-layer edge
nt	= nonturbulent
$t$	= turbulent
$w$	= wall condition
0	= stagnation condition

## Introduction

THE study of high-speed transition is very important for the efficient design of hypersonic vehicles such as the X-33, X-34, and other reusable launch vehicles. Important design parameters, such as skin friction and heat transfer, are increasing rapidly or are maximum within the transitional region. The inability to predict accurately transition onset and extent on hypersonic vehicles has been an impediment to designing low-cost space transportation systems.

The purpose of this investigation is to address this area of research by adapting a newly developed approach for transitional onset prediction<sup>1</sup> to high-speed flows. The approach of Ref. 1 treats transitional flows in a turbulence-like manner. It is based on the fact that exact equations governing fluctuations are the same irrespective of their nature. To implement this approach, it is necessary to model correlations in the equations that govern the fluctuations in such a way so as not to invoke the nature of fluctuations. This modeling is accomplished by formulating a two-equation model that governs the variance of velocity (i.e., the kinetic energy of the fluctuations  $k$ ) and the variance of vorticity (i.e., enstrophy  $\zeta$ ). To date, the relationship between the transition/turbulent stress and the strain rate has been described by the Boussinesq approximation, with differences in transitional and turbulent flows relating to eddy viscosity and fluctuation timescales. For turbulent flows traditional concepts have been used,<sup>2,3</sup> whereas for nonturbulent fluctuations scaling arguments based on linear stability theory have been employed.<sup>1,4–9</sup> As different scaling arguments can hold for different types of transition processes, the current method is not mechanism-independent, such as is the case for empirical correlations. Rather, it is dictated by the dominant mode of instability growth and the manner in which it is influenced by environmental factors such as freestream fluctuation intensity and surface roughness. This information can be gleaned from linear stability theory or experiment.<sup>10</sup>

The bridging of the nonturbulent and turbulent solutions is currently accomplished by the Dhawan–Narasimha intermittency expression.<sup>11</sup> This bridging requires the specification of a transition point that can be selected as the streamwise location at which skin friction, heat transfer, or recovery factor first attains a local

Presented as Paper 99-3792 at the AIAA 30th Fluid Dynamics Conference, Norfolk, VA, 28 June–1 July 1999; received 22 July 1999; revision received 6 January 2000; accepted for publication 7 January 2000. Copyright © 2000 by the American Institute of Aeronautics and Astronautics, Inc. All rights reserved.

\*Research Assistant, Mechanical and Aerospace Engineering. Student Member AIAA.

†Aerospace Engineer, Missile Systems Division. Member AIAA.

‡Professor, Mechanical and Aerospace Engineering. Associate Fellow AIAA.

minimum. Using this basic idea, successful simulations of transitional flows driven by Tollmien-Schlichting, crossflow, or free shear-layer instabilities have been conducted.<sup>1,4-9</sup> This has been accomplished using available computational fluid dynamics (CFD) codes and without having to use stability codes.

In the present work three different sets of experiments involving flared and straight cones were utilized to validate the approach. The first set of data was obtained by Chen et al.<sup>12</sup> in the NASA Langley Research Center Mach 3.5 Pilot Low-Disturbance Tunnel, using a 5-deg half-angle sharp straight cone. The second set is that of Lachowicz et al.<sup>13,14</sup> and Blanchard and Selby<sup>15</sup> conducted in the NASA Langley Research Center Mach 6 Quiet Tunnel<sup>16</sup> using different 5-deg sharp flared cones. The last set is that of Kimmel<sup>17</sup> carried out in the Arnold Engineering Development Center (AEDC) Tunnel B using straight and flared cones.

## Formulation of the Problem

### Approach

The model to be used in this study is an extension of the transition/turbulence model,<sup>1</sup> which treats nonturbulent fluctuations in a turbulence like manner. Traditionally, the transition problem has been treated as a combination of two problems. The first deals with the transition extent given the onset, whereas the second deals with the transition onset. One of the methods employed in calculating the extent is to replace the turbulent viscosity by

$$\Gamma \mu_t \quad (1)$$

where  $\Gamma$  is the fraction of the time the flow is turbulent at a given location.  $\Gamma$  varies from 0, at onset, to 1 when the transition to turbulence is complete. The most widely used expression for  $\Gamma$  is that of Dhawan and Narasimha.<sup>11</sup> There are many methods that can be used to specify transition onset: selection based on experiment, experimental correlation, or use of stability theory. Methods based on stability theory employ the  $e^n$  method or a method based on the parabolized stability equations (PSE).

Even when transition onset is specified from experimental results, Eq. (1) does not perform well. One of the reasons for this behavior is because the preceding formula does not account for the nonturbulent fluctuations that eventually lead to transition. This result led Young et al.<sup>18</sup> and Warren et al.<sup>19</sup> to replace  $\mu_t$  by

$$(1 - \Gamma)\mu_{nt} + \Gamma \mu_t \quad (2)$$

where  $\mu_{nt}$  represents the contribution of the nonturbulent fluctuations and is derived using results from linear stability theory. In the work of Refs. 18 and 19, the onset was assumed.

In the present investigation the constitutive stress-strain relations for the nonturbulent fluctuations are derived from observed or computed characteristics of first- and second-mode instabilities. Because mechanisms responsible for transition are different for the two types of instabilities, corresponding stress-strain relations are different. In both cases, however,  $\mu_{nt}$  is set as

$$\mu_{nt} = C_\mu \rho k \tau_{nt}, \quad C_\mu = 0.09 \quad (3)$$

The turbulence model is based on the  $k$ - $\zeta$  model of Robinson and Hassan.<sup>3</sup> This model is free of damping and wall functions and is coordinate independent. Further, all modeled correlations are tensorially consistent and Galilean invariant. The model reproduces the correct growth rates of all free shear layers and is capable of predicting separated flow in the presence and absence of shocks. The model also incorporates relevant compressibility effects and has been demonstrated for both two- and three-dimensional separated flows where Morkovin's hypothesis is expected to hold.

### Transition from First-Mode Disturbances

For moderate supersonic Mach numbers, below approximately four, the dominant mode of instability is the oblique first mode. First-mode disturbances are vorticity disturbances that are characterized by fluctuations in velocity. Two-dimensional first-mode disturbances in low-speed flows are known as Tollmien-Schlichting waves. For this case  $\tau$  is chosen as<sup>1</sup>

$$\tau_1 = a/\omega \quad (4)$$

where  $a$  is a model constant that depends on the freestream intensity  $Tu$  defined as

$$Tu = 100\sqrt{\frac{2}{3}(k_\infty | Q_\infty^2)} \quad (5)$$

where  $k_\infty$  and  $Q_\infty$  are the freestream kinetic energy of the fluctuations and magnitude of freestream velocity. The model constant has the form<sup>1</sup>

$$a = 0.069(Tu - 0.138)^2 + 0.00819 \quad (6)$$

The quantity  $\omega$  is the frequency of the first-mode disturbance having the maximum amplification rate and is given by a correlation developed by Walker<sup>20</sup> as

$$\omega v / Q_e^2 = 3.2 Re_{\delta^*}^{-\frac{3}{2}} \quad (7)$$

where  $Re_{\delta^*}$  is the edge Reynolds number based on the displacement thickness  $\delta^*$ . The preceding correlation is based on results of stability calculations for Falkner-Skan profiles obtained by Obremski et al.<sup>21</sup> and is suited for flows where the pressure gradient is not necessarily zero.

For high-speed flows Eqs. (4) and (7) are modified in two different ways. The first is to allow for compressibility effects. Following Warren et al.,<sup>18</sup> a reference temperature  $T^*$  determined as

$$T^*/T_e = 1 + 0.032M_e^2 + 0.56(T_w/T_e - 1) \quad (8)$$

is used to calculate  $v$  in Eq. (7). The second modification is to allow for the oblique modes, which is accomplished in this work by dividing the expression in Eq. (4) by  $(\cos \psi)^{1/2}$ , where  $\psi$  is the angle between the wave-number vector and the freestream. This choice reduces to the two-dimensional mode when  $\psi = 0$  and was arrived at by numerical optimization. Estimates of  $\psi$  are taken from Fig. 10.11 of Ref. 22.

### Second-Mode Disturbances

At Mach numbers higher than four, the transition process is dominated by second-mode disturbances. Second-mode disturbances are acoustical disturbances characterized by large fluctuations in pressure and temperature and are much larger than velocity fluctuations. As the boundary-layer edge Mach number increases above 2.2, a region of the boundary layer becomes supersonic relative to the phase velocity. Mack<sup>22</sup> showed that when such a situation exists multiple solutions to the inviscid stability equation arise. These additional solutions are called the higher modes. The second mode is the most unstable of these higher modes. For this mode  $\tau$  is chosen as

$$\tau_2 = b/\omega_{sm} \quad (9)$$

with

$$\omega_{sm} \approx U_p/\lambda \quad (10)$$

where  $U_p$  is about 0.94 times the edge velocity.  $\lambda$  is approximately  $2\delta$ .

The total transitional contribution to the viscosity timescale is set as the sum of the contributions from the first and second modes:

$$\tau_{nt} = \tau_1 + \tau_2 \quad (11)$$

Similarly, the decay time  $\tau_k$  (Ref. 1) for the turbulent kinetic energy is modeled using contribution from nonturbulent and turbulent fluctuation as

$$1/\tau_k = (1 - \Gamma)/\tau_{k,nt} + \Gamma/\tau_{k,t} \quad (12)$$

$$1/\tau_{k,nt} = (a + b)(v_t/v)s, \quad 1/\tau_{k,t} = k/v\zeta \quad (13)$$

where

$$s^2 = \tilde{s}_{ij}\tilde{s}_{ij}, \quad \tilde{s}_{ij} = \left(\frac{1}{2}\right)\left(\frac{\partial \tilde{u}_i}{\partial x_j} + \frac{\partial \tilde{u}_j}{\partial x_i}\right) \quad (14)$$

### Intermittency and Onset Prediction Criteria

The intermittency  $\Gamma$  is given by Dhawan and Narasimha's expression<sup>11</sup> as

$$\Gamma(x) = 1 - \exp(-0.412\xi^2) \quad (15)$$

with

$$\xi = \max(x - x_t, 0)/\alpha \quad (16)$$

and  $\alpha$  is a characteristic extent of the transitional region. An experimental correlation (20) between  $\alpha$  and  $x_t$  is

$$Re_\alpha = 9.0Re_{x_t}^{0.75} \quad (17)$$

with  $x_t$  being the location where turbulent spots first appear, or the onset of transition. In this work onset is determined as part of the solution.

A number of criteria may be used to determine transition onset.<sup>1</sup> The criteria can be one of the following: minimum skin friction, minimum heat transfer, or minimum recovery factor (adiabatic walls). Further, it was shown in Ref. 1 that a transition onset criterion based on the nonturbulent eddy viscosity correlates well with minimum skin-friction criterion for flat plates and airfoils. According to this criterion, onset is determined by the requirement

$$R_T = (1/C_\mu)(v_{nt}/v) = 1 \quad (18)$$

The need to develop a criterion like this was a result of the fact that during the transient phase of a Navier–Stokes calculation surface derivatives have a tendency to fluctuate, and this fluctuation can delay or prevent convergence. It was found in Ref. 1 that the expression indicated in Eq. (18) was more forgiving and, in addition, gave accurate results.

The criteria of minimum skin friction and minimum heat transfer are valid for simple shapes such as flat plates and cones in the absence of adverse pressure gradient. For supersonic flow wall skin friction increases in the presence of adverse pressure gradients.<sup>23</sup> Similar behavior is observed for heat transfer. Thus, if one considers flared cones, such as the case for  $M = 6$  experiments, then the criterion of minimum skin friction will not yield meaningful results if the transition takes place on the curved surface of the cone. In this case a criterion such as that indicated in Eq. (18) is more meaningful. On the other hand, if the transition takes place on the straight part of a flared cone such as was the case for  $M = 8$ , then minimum heat-transfer criterion is meaningful.

### Model Constants

Intensity is not measured at hypersonic Mach numbers. Instead, the rms of mass flux  $\tilde{m}$  over the mean mass flux  $\bar{m}$  is measured. For low-speed flows this ratio reduces to the intensity. Thus, for present purposes  $\tilde{m}/\bar{m}$  is a measure of the intensity.

The model constant appearing in Eq. (6) was correlated in Ref. 1 for flows where natural transition is expected to take place. Thus, the correlation is suited for studying flows in quiet tunnels such as the NASA Langley Research Center  $M = 3.5$  and  $M = 6$  tunnels. The AEDC Tunnel B is not a quiet tunnel in terms of freestream intensity levels. Donaldson and Coulter<sup>24</sup> reported values of intensity ranging from 1.5 to 3.8% for  $M = 8$  and a range of Reynolds numbers. Because only a small portion of the spectrum is in the second-mode frequency range (frequencies more than 80–100 kHz), Stetson and Kimmel<sup>25</sup> suggested that a conventional hypersonic wind tunnel can be quiet for second-mode disturbances and noisy for first-mode disturbances.

The  $M = 3.5$  experiments are dominated by oblique first mode, and values of  $b \leq 3a$  had little or no effects on the calculated recovery factors and transition onset. Based on results of linear stability theory, the experiments at  $M = 6$  and 8 are dominated by the second mode. The model constant  $b$  for the  $M = 6$  experiments was correlated in terms of the model constant  $a$  using the onset criterion indicated in Eq. (18). Because of the high intensity levels in Tunnel B, it is not possible to relate  $b$  to the constant  $a$  that was developed for low intensity levels. Thus, both  $a$  and  $b$  for the  $M = 8$

data were correlated by comparing with the data of Ref. 17 using a minimum heat flux criterion. Because of the different onset criteria employed, the resulting  $a$  and  $b$  values are not the same for the two sets of hypersonic Mach numbers.

### Numerical Method

The modeling proposed here has been incorporated into Olynick and Hassan's<sup>26</sup> two-dimensional/axisymmetric implicit solver for hypersonic flows. This algorithm solves the governing equations for five-species air in thermochemical nonequilibrium. The solver uses Roe's flux-differencesplitting<sup>27</sup> for the inviscid flux, extended to higher order using MUSCL variable extrapolation<sup>28</sup> with a minmod slope limiter. Time integration is accomplished using the diagonal implicit variant of Yoon and Jameson's lower-upper symmetric Gauss–Seidel method,<sup>29</sup> which only requires the inversion of diagonal matrices. This feature is attractive for nonequilibrium flows, where a large number of partial differential equations must be solved.

Because the current flowfields under investigation are approximately perfect-gas flows, vibrational relaxation and chemical reactions are disabled to obtain the results in this study. Additionally, the high-temperature transport-property calculations originally used in the code were replaced with Sutherland's law for viscosity and a constant laminar Prandtl number of 0.72. Closure for the Favre-averaged energy equation is accomplished using a constant turbulent Prandtl number of 0.89.

### Results and Discussion

To validate the current approach, three test cases involving straight and flared cones were considered. Two cases were conducted in quiet tunnels, whereas the third was conducted in a conventional hypersonic tunnel. None of the experiments measured onset or extent of transition, they were inferred from heat transfer and recovery factor measurements. Thus, predictions of the theory are compared with recovery factors for the  $M = 3.5$  test cases, with adiabatic wall temperatures for the  $M = 6$  cases and with heat-transfer rates for the  $M = 8$  cases. All cases considered assume zero angle of attack.

Because the theory of Ref. 1 and current extension are suited for the study of natural transition, model constants suited for the  $M = 3.5$  and 6 experiments are not expected to yield correct transition onset predictions in conventional hypersonic tunnels. This is because the correlation for  $a$  indicated in Eq. (6) is limited to values of  $Tu \leq 0.5$ .

Two of the sets of experiments were the subject of an earlier investigation in Ref. 19. Grids as high as  $275 \times 75$  (along and normal to the surface) were investigated there and here. Grids used in the results presented here are indicated next for each test case considered.

### $M = 3.5$ Test Cases

The measurements of Chen et al.<sup>12</sup> were carried out in the NASA Langley Research Center Mach 3.5 Pilot Low-Disturbance Tunnel using 5-deg half-angle cones. Three cases from these experiments were selected for this investigation. All of the cases have the same Mach number but different stagnation pressures resulting in the following unit Reynolds numbers:

$$\text{Flow 3, case 5, } Re/L = 7.8 \times 10^7/\text{m}$$

$$\text{Flow 3, case 6, } Re/L = 5.89 \times 10^7/\text{m}$$

$$\text{Flow 3, case 7, } Re/L = 3.85 \times 10^7/\text{m}$$

The boundary-layer conditions for all cases were  $Me = 3.36$ ,  $T_e = 98$  K, and  $Tu = 0.1$ , as reported by Singer et al.<sup>30</sup>

Figures 1–3 compare the prediction of the theory with experiment. The grid employed is  $252 \times 75$ . For these calculations the first-mode contribution to the nonturbulent timescale is given by

$$\tau_1 = a/\omega \cdot (\cos \psi)^{\frac{1}{2}} \quad (19)$$

with  $\psi$ , the angle between the wave-number vector and the freestream, determined from Fig. 10.11 of Ref. 22 as 63 deg. One

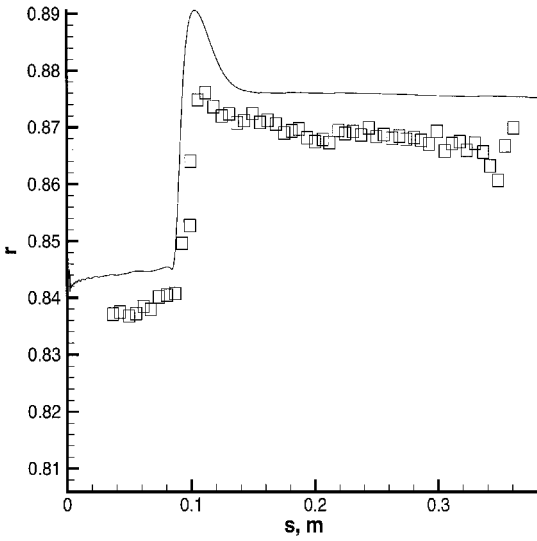


Fig. 1 Measured and computed recovery factor:  $M = 3.5$  and  $Re/L = 7.8 \times 10^7/m$ .

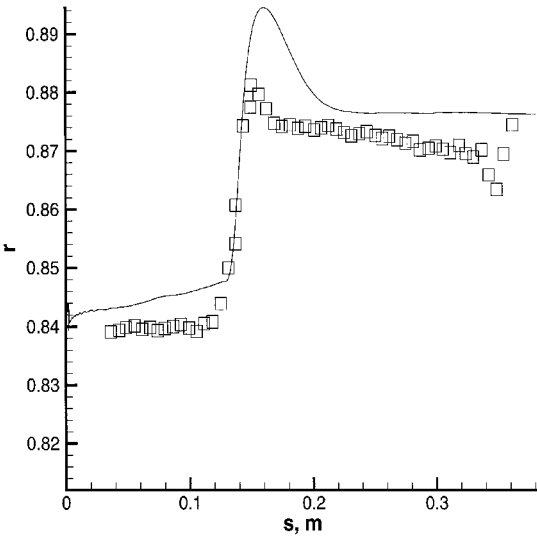


Fig. 2 Measured and computed recovery factor:  $M = 3.5$  and  $Re/L = 5.89 \times 10^7/m$ .

recovers the normal mode expression given by Eq. (4) when  $\psi = 0$ . Onset is determined by the minimum skin-friction criterion. In general, good agreement with experiment is indicated. The contribution of the second mode was investigated. For

$$b \leq 3a \quad (20)$$

the second mode had minimal effects on the results shown in Figs. 1–3. The measured recovery factors in the turbulent region are lower than indicated by an earlier measurement by Mack<sup>31</sup> over cones at Mach numbers varying from 1.2 to 6.0 (Fig. 7.25 in Ref. 32).

#### $M = 6$ Test Cases

The usable quiet core length in the  $M = 6$  tunnel was about 0.63 m (25 in.). This necessitated the use of flared cones to produce an adverse pressure gradient in order to produce measurable disturbance growth in the boundary layer. The flare design resulted in an approximately constant boundary-layer thickness and allowed the second-mode disturbance to grow. Two cones were tested in this facility. The first<sup>13,14</sup> was a 0.508-m (20-in.), 5-deg half-angle cone with the straight surface extending 0.254 m (10 in.); the flared surface has a radius of curvature of 2.36 m (93.07 in.). Transition was observed on the sharp version of the cone, and this is the geometry employed in this study. The second cone<sup>15</sup> was a 0.457-m (18-in.), 5-deg half-angle cone with the straight section extending 0.152 m

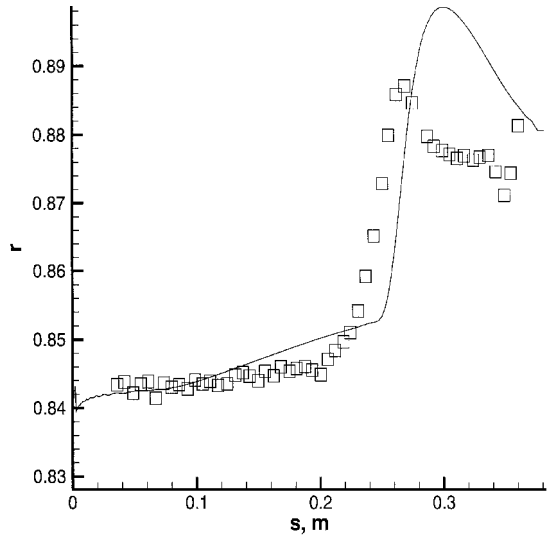


Fig. 3 Measured and computed recovery factor:  $M = 3.5$  and  $Re/L = 3.85 \times 10^7/m$ .

(6 in.) with a flare radius of 2.34 m (91.94 in.). Only the adiabatic case was considered for this geometry. In both cases the stagnation pressure  $P_0$  and temperature  $T_0$  were 896.32 kPa (130 psia) and 450 K (810°R), respectively. In both investigations second-mode instability was deemed to be that responsible for transition.

Both experiments presented a major challenge because of the apparent inconsistency in the experimental data. Assuming  $T_0$  to be 450 K, measurements indicated in Ref. 13 (Fig. 23), which shows a maximum adiabatic wall temperature of 415.6 K, do not match measurements shown in other figures, which indicate a maximum adiabatic wall temperature of 432.2 K and a maximum recovery factor of 0.96. Similar remarks hold for the adiabatic wall temperature measurement in Ref. 15, which measure a peak wall temperature of about 448.3 K. This results in a recovery factor in excess of 0.97. It is true that the edge Mach number decreases in the presence of adverse pressure gradients, but that should not affect values of recovery factor, which is defined as

$$r = \frac{T_{aw} - T_e}{T_0 - T_e}$$

where

$$T_{aw} = T_e \left\{ 1 + [(\gamma - 1)/2] r M_e^2 \right\}, \quad T_0 = T_e \left\{ 1 + [(\gamma - 1)/2] M_e^2 \right\}$$

Thus, without knowing the details of how the experiments were conducted, it is not obvious how one would explain these high values of the recovery factors.

Because the skin friction increases in the presence of adverse pressure gradients for hypersonic Mach numbers, use of a minimum skin-friction criterion to determine transition onset is not an option. Therefore, results presented in Figs. 4 and 5 employed the condition indicated in Eq. (18) to determine  $x_T$ .

Although transition was attributed in Refs. 13–15 to the growth of the second mode, we were unable to determine model constant  $b$  without inclusion of the contributions of the first mode. In other words, if the contribution of the first mode is set to zero, then values of  $b$  will either result in no transition or transition on the straight part of the cone.

Balakumar and Malik<sup>33</sup> showed that the growth rates for the first and second modes are comparable. This may explain the need to allow for contributions from both modes to arrive at a transition model. Further support to allow for contribution of the two modes follows from Refs. 13 and 14 (Figs. 23 and 2), which show that transition onset is not the same when the  $M = 6$  tunnel is operated in conventional and quiet modes. If the second mode were the only mode contributing to transition, then one would expect that transition onset would be independent of intensity.

A mode constant  $b = 0.054$  ( $6.5a$ ) is used in the results indicated in Figs. 4 and 5. Both calculations employed a grid of  $160 \times 80$  and

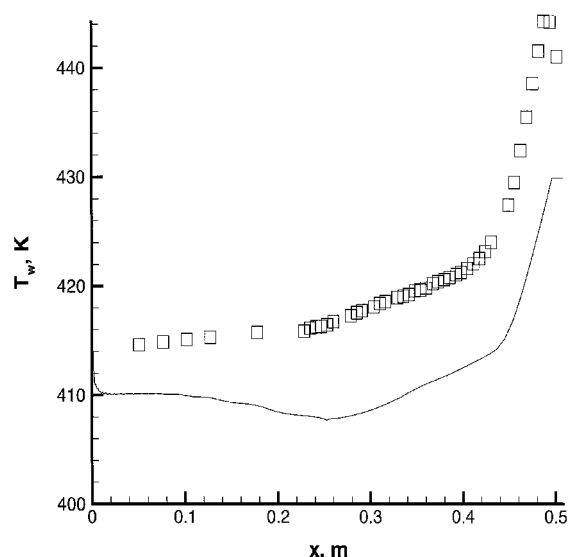


Fig. 4 Measured and computed adiabatic wall temperature:  $M = 6.0$ , 0.508-m (20-in.) flared cone.

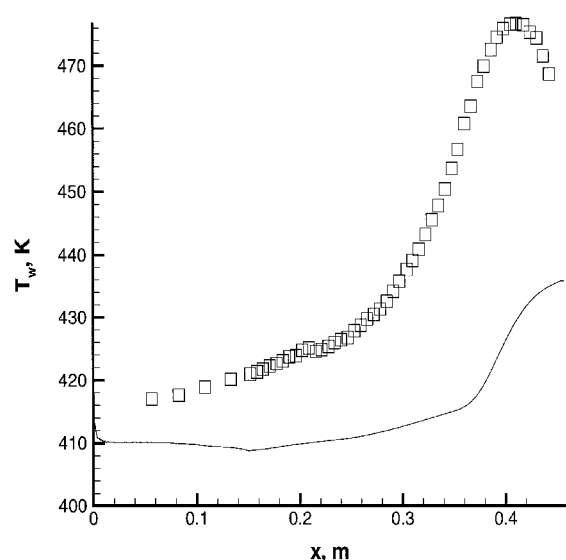


Fig. 5 Measured and computed adiabatic wall temperature:  $M = 6.0$ , 0.457-m (18-in.) flared cone.

an intensity  $Tu = 0.1$ . In spite of the difficulties associated with adiabatic wall temperature, excellent agreement with pressure measurements was obtained. Moreover, growth rate data in Ref. 15 suggest that transition onset starts at about  $x = 0.356$  m (14 in.), which is consistent with current findings.

#### $M = 8$ Test Cases

Because a theory developed for natural transition is not suited to model experiments carried out in conventional wind tunnels, the goal here is to determine whether a transition mechanism based on the second mode will yield reasonable agreement with experiment. The value of intensity was not provided, and a value of 1.5% is assumed. It quickly became evident that such a goal cannot be achieved. In view of the results just indicated for  $M = 6$  operation in quiet and conventional modes, this result is to be expected. Thus the model developed below allows for contributions from both modes. Because of the high levels of freestream intensities, a criterion based on Eq. (18) is meaningless. Thus, an onset criterion based on a minimum heat transfer is employed.

Two 7-deg half-angle cones were considered in this investigation: a straight cone and a flared cone characterized by  $dP/dx = 4$ . This corresponds to the nondimensional pressure gradient parameter  $(L/C_{pe})(dC_p/dx)$ , where  $L$  is the cone length and  $C_{pe}$  is the

pressure coefficient on the conical forebody. For the two cases considered,  $Re/L = 6.562 \times 10^6/m$ , the length is 1.016 m (40 in.), and the wall temperature is 300 K. The grid employed is  $201 \times 91$ .

Figures 6 and 7 compare the predictions of the theory for sharp and flared cases. The model constants, which are obtained by numerical optimization, are  $a = 0.016$  and  $b = 0.01$ . The scatter in the data ( $\pm 10\%$  accuracy) makes it difficult to determine the role of adverse pressure gradient on the measurements. Theory indicates an earlier transition of the flared case. Further, the underprediction of the heat flux in the turbulent region may be a result of the assumed intensity.

Both  $a$  and  $b$  are intensity dependent. Because the freestream intensity is in the bypass region, there is a question whether a general theory based on first- and second-mode scaling is viable for flows in conventional wind tunnels. More measurements at various intensities are needed to resolve this question.

Current results were obtained using a typical Navier-Stokes solver that employs a two-equation turbulence model. The cost of the calculation is comparable to that of a fully turbulent flow. This approach may be compared with  $e''$ -methods, which require either Euler and boundary-layer codes or Navier-Stokes codes with higher resolution in order to generate accurate mean flows with smooth second derivatives, a stability code, specification of mode frequencies, and the value of  $n$  in order to determine transition onset. Moreover, the procedure has never been dynamically coupled to a flow solver to obtain the complete flowfield.

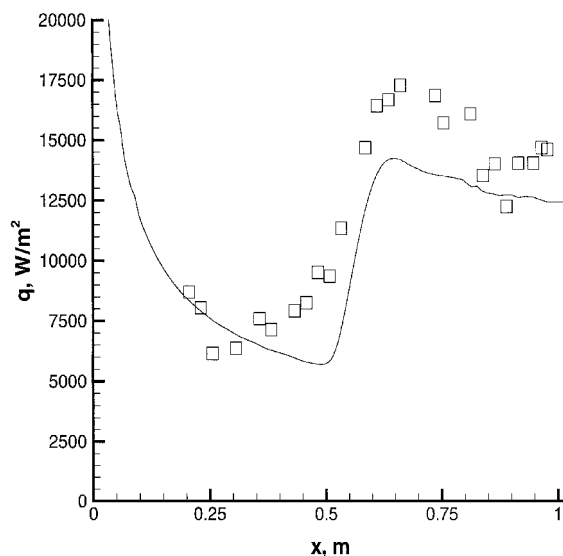


Fig. 6 Measured and computed heat flux:  $M = 8.0$ , straight cone.

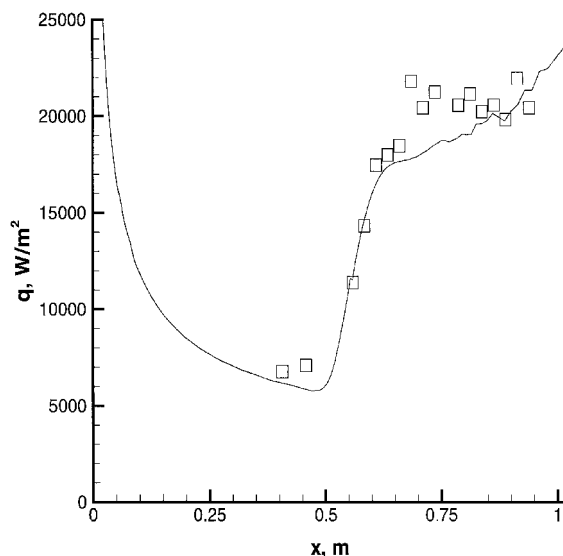


Fig. 7 Measured and computed heat flux:  $M = 8.0$ , flared cone.

## Conclusion

The existing  $k$ - $\zeta$  transition/turbulent model developed by Warren and Hassan<sup>1</sup> can be extended to high Mach-number flows. Reasonable predictions of transition onset were indicated. Further, with the exception of the  $M = 6$  data, fair to good agreement with experiment is obtained.

The work further confirms that treating transitional flows in a turbulence-like manner is a viable way of describing such flows.

The cost of calculating the entire flowfield is less than calculating the mean laminar flow in the  $e^n$ -method because stability codes require flow properties with smooth second derivatives, which necessitates a much finer grid.

Finally, there is a need to conduct experiments designed to determine onset and extent of transition in quiet tunnels. Such experiments would be of great use for code calibration and validation.

## Acknowledgments

This work is supported in part by NASA Grant NGT-1-52177 and Sandia National Laboratories Grant BF-0856. Computer resources were provided by the North Carolina Supercomputing Center. The authors would like to acknowledge many helpful discussions with Ndaona Chokani.

## References

- <sup>1</sup>Warren, E. S., and Hassan, H. A., "Transition Closure Model for Predicting Transition Onset," *Journal of Aircraft*, Vol. 35, No. 5, 1998, pp. 769-775.
- <sup>2</sup>Robinson, D. F., Harris, J. E., and Hassan, H. A., "Unified Turbulence Closure Model for Axisymmetric and Planar Free Shear Flows," *AIAA Journal*, Vol. 33, No. 12, 1995, pp. 2324-2331.
- <sup>3</sup>Robinson, D. F., and Hassan, H. A., "Further Development of the  $k$ - $\zeta$  (Enstrophy) Turbulence Closure Model," *AIAA Journal*, Vol. 36, No. 10, 1998, pp. 1825-1833.
- <sup>4</sup>Warren, E. S., and Hassan, H. A., "An Alternative to the  $e^n$ -Method for Determining Onset of Transition," AIAA Paper 97-0825, Jan. 1997.
- <sup>5</sup>Warren, E. S., and Hassan, H. A., "A Transition Model for Swept Wing Flows," AIAA Paper 97-2245, June 1997.
- <sup>6</sup>Nance, R. P., Horvath, T. J., and Hassan, H. A., "Transition and Turbulence Modeling for Blunt-Body Wake Flows," AIAA Paper 97-2570, Jan. 1997.
- <sup>7</sup>Nance, R. P., Hollis, B. R., Horvath, T. J., and Hassan, H. A., "Solution of Transitional Wake Flows at Mach 10," AIAA Paper 98-2939, June 1998.
- <sup>8</sup>Nance, R. P., Hollis, B. R., Horvath, T. J., Alter, S. J., and Hassan, H. A., "Computational Study of Hypersonic Transitional Wake Flows," *Journal of Thermophysics and Heat Transfer*, Vol. 13, No. 2, 1999, pp. 236-242.
- <sup>9</sup>Czerwicz, R. M., Edwards, J. R., Rumsey, C. L., Bertelrud, A., and Hassan, H. A., "Study of High-Lift Configurations Using  $k$ - $\zeta$  Transition/Turbulence Model," AIAA Paper 99-3186, June 1999.
- <sup>10</sup>Reed, H. L., Haynes, T. S., and Saric, W. S., "Computational Fluid Dynamic Validation Issues in Transition Modeling," *AIAA Journal*, Vol. 36, No. 5, 1998, pp. 742-751.
- <sup>11</sup>Dhawan, S., and Narasimha, R., "Some Properties of Boundary-Layer Flow During Transition from Laminar to Turbulent Motion," *Journal of Fluid Mechanics*, Vol. 3, No. 4, 1958, pp. 414-436.
- <sup>12</sup>Chen, F.-J., Malik, M. R., and Beckwith, I. E., "Boundary-Layer Transition on a Cone and Flat Plate at Mach 3.5," *AIAA Journal*, Vol. 27, No. 6, 1989, pp. 687-693.
- <sup>13</sup>Lachowicz, J. T., and Chokani, N., "Hypersonic Boundary-Layer Stability Experiments in a Quiet Wind Tunnel with Bluntness Effects," NASA CR 198272, Jan. 1996.
- <sup>14</sup>Lachowicz, J. T., Chokani, N., and Wilkinson, S. P., "Boundary-Layer Stability Measurements in Hypersonic Quiet Tunnel," *AIAA Journal*, Vol. 34, No. 12, 1996, pp. 2496-2500.
- <sup>15</sup>Blanchard, A. E., and Selby, G. V., "An Experimental Investigation of Wall-Cooling Effects on Hypersonic Boundary-Layer Stability in a Quiet Wind Tunnel," NASA CR 198287, Feb. 1996.
- <sup>16</sup>Blanchard, A. E., Lachowicz, J. T., and Wilkinson, S. P., "NASA Langley Mach 6 Quiet Wind-Tunnel Performance," *AIAA Journal*, Vol. 35, No. 1, 1997, pp. 23-28.
- <sup>17</sup>Kimmel, R. L., "The Effects of Pressure Gradients on Transition Zone Length in Hypersonic Boundary Layers," *Journal of Fluids Engineering*, Vol. 119, No. 1, 1997, pp. 36-41.
- <sup>18</sup>Young, T. W., Warren, E. S., Harris, J. E., and Hassan, H. A., "New Approach for the Calculation of Transitional Flows," *AIAA Journal*, Vol. 31, No. 4, 1993, pp. 629-636.
- <sup>19</sup>Warren, E. S., Harris, J. E., and Hassan, H. A., "Transition Model for High-Speed Flow," *AIAA Journal*, Vol. 33, No. 8, 1995, pp. 1391-1397.
- <sup>20</sup>Walker, G. J., "Transitional Flow on Axial Turbomachine Blading," *AIAA Journal*, Vol. 27, No. 5, 1989, pp. 595-602.
- <sup>21</sup>Obremski, H. J., Morkovin, M. V., and Landahl, M., "Portfolio of Stability Characteristics of Incompressible Boundary-Layers," AGARDograph 134, March 1969.
- <sup>22</sup>Mack, L. M., "Boundary-Layer Linear Stability Theory," AGARD Rept. 709, June 1986.
- <sup>23</sup>Fernando, E. M., and Smits, A. J., "A Supersonic Turbulent Boundary-Layer in an Adverse Pressure Gradient," *Journal of Fluid Mechanics*, Vol. 211, Pt. 1, 1990, pp. 285-307.
- <sup>24</sup>Donaldson, J., and Coulter, S., "A Review of Free-Stream Flow Fluctuation and Steady-State Flow Quality Measurements in the AEDC/VKF Supersonic Tunnel A and Hypersonic Tunnel B," AIAA Paper 95-6137, April 1995.
- <sup>25</sup>Stetson, K. F., and Kimmel, R. L., "On Hypersonic Boundary-Layer Stability," AIAA Paper 92-0737, Jan. 1992.
- <sup>26</sup>Olynick, D. P., and Hassan, H. A., "A New Two-Temperature Dissociation Model for Reacting Flows," *Journal of Thermophysics and Heat Transfer*, Vol. 7, No. 4, 1993, pp. 687-696.
- <sup>27</sup>Roe, P. L., "Approximate Riemann Solvers, Parameter Vectors and Difference Schemes," *Journal of Computational Physics*, Vol. 43, No. 2, 1981, pp. 357-372.
- <sup>28</sup>van Leer, B., "Towards the Ultimate Conservative Difference Scheme, V. A Second Order Sequel to Godunov's Method," *Journal of Computational Physics*, Vol. 32, No. 1, 1979, pp. 263-275.
- <sup>29</sup>Yoon, S., and Jameson, A., "An LU-SSOR Scheme for the Euler and Navier-Stokes Equations," AIAA Paper 87-0600, Jan. 1987.
- <sup>30</sup>Singer, B. A., Dinavahi, S. P. G., and Iyer, V., "Testing of Transition Region Models: Test Cases and Data," NASA CR 4371, May 1991.
- <sup>31</sup>Mack, L. M., "An Experimental Investigation of the Temperature Recovery Factor," California Inst. of Technology, Rept. 20-80, Pasadena, CA, 1954.
- <sup>32</sup>White, F. M., *Viscous Fluid Flow*, 2nd ed., McGraw-Hill, New York, 1991, p. 555.
- <sup>33</sup>Balakumar, P., and Malik, M. R., "Effect of Adverse Pressure Gradient and Wall Cooling on Instability of Hypersonic Boundary Layers," High Technology, Rept. HTC-9404, Hampton, VA, March 1994.

M. Torres  
Associate Editor